Insights into agricultural influences and weathering processes from major ion patters in the Wiesent River catchment (Germany)

Robert van Geldern[1,*], Peter Schulte[1,2], Michael Mader[1], Alfons Baier[1], Johannes A.C. Barth[1], Kern Lee[1]

[1] *Friedrich-Alexander-University Erlangen-Nuremberg (FAU), Department of Geography and Earth Sciences, GeoZentrum Nordbayern, Schlossgarten 5, 91054 Erlangen, Germany*

[2] *Gehrenhagweg 6, CH-5420 Ehrendingen, Switzerland*

for submission to

Hydrological Processes

*Corresponding author.

robert.van.geldern@fau.de. phone +49 9131 8522514. fax +49 9131 29294.

This is the initial submitted version that has not undergo peer-review, revision, and final proof reading of the following article:

van Geldern, R., Schulte, P., Mader, M., Baier, A., Barth, J.A.C., Juhlke, T.R. and Lee, K. (2018): Insights into agricultural influences and weathering processes from major ion patterns. - Hydrological Processes, 32, 891-903,

which has been published in final revised and accepted form at http://dx.doi.org/10.1002/hyp.11461.

ABSTRACT

A study of the geochemical downriver evolution of the Wiesent River and its tributaries revealed unexpected decreases of nitrate downstream from the source, with maximum values of 31.6 mg L^{-1} to minimum values of 10 mg L^{-1} near the mouth. This trend persisted over the length of the river even though increased agricultural activities are evident in the downstream section of the catchment. This pattern is caused by fertilizer inputs via fast fracture flow and fast conduits from karst lithology in the upstream area that may have reached the river's source even from beyond the hydrological catchment boundaries. Further downstream, these influences became diluted by tributary inputs that drain subcatchments dominated by claystone and sandstone lithologies that increased potassium and sulfate concentrations. In addition, except for inputs in the source area, groundwater contributions along the river course were found to be minor as attested by seasonal temperature trends of the river, with values ranging from 18.9 °C during summer to 0.9 °C during winter. This seasonality was absent at the source where water temperatures were consistently 9 °C throughout the year, which is a typical value for central European groundwater.

KEYWORDS

watershed, hydrology, geochemistry, weathering, karst, fertilizers

INTRODUCTION

The downriver evolution of various river systems has been examined in several studies worldwide (Meybeck, 1982; Meybeck, 1993; Yang *et al.*, 1996; Richey *et al.*, 2002). Most of these were aimed at weathering processes and continental fluxes of major element and carbon phases. Following these studies, work on smaller river systems were also carried out (Barth *et al.*, 2003; Kanduč *et al.*, 2007; Stögbauer *et al.*, 2008; Brunet *et al.*, 2011), and most of these showed increasing conductivities and fluxes with closer proximity to confluences to larger river systems. This trend corresponds to increasing element loads further downstream and is usually related to increasing anthropogenic activities including traffic infrastructure, settlements and agricultural practices in the downstream sections of catchments.

Here we present a small river system of 72.4 km length, the Wiesent River (Figure 1). Being dominated by karst lithology, it was first studied as an ideal natural laboratory for investigations of the aqueous carbon cycle in karst areas and its response to excessive carbon loss to the atmosphere, particularly in its source area (van Geldern *et al.*, 2015). The catchment is situated in a dolomite and calcite-dominated terrain that trends towards shale and sandstone terrains in the lower reaches of the river. This allows for interpretations of spatial heterogeneity in river water chemistry, while sampling over almost one year enabled temporal interpretations of seasonal variations in riverine solutes, carbon transport, CO_2 evasion and associated changes in the carbon isotope distribution of dissolved inorganic carbon (DIC). The Wiesent River is also influenced by anthropogenic activities including farming, fish farming and tourism. In particular, farming activities along the river course were expected to significantly influence the water chemistry. These influences may be stronger in a karst-dominated lithology as compared to catchments with clastic sediments, due to the fast conduit systems present in karst. These conduits also make karst aquifers highly vulnerable to

anthropogenic pollution because of the virtual absence of filter effects that are common in pore aquifers. Moreover, it is known that fertilizers can lower pH values and thus cause additional weathering that should, in turn, be particularly pronounced in karst that is susceptible to acidity changes (Perrin *et al.*, 2008; Gandois *et al.*, 2011).

The objectives of this study were to assess the spatial and temporal downriver evolution of major ion chemistry in a typical karst river. Specifically, we investigated whether the hypothesized continuous increase of solutes along the flow path of the river could be observed. With this in mind, we evaluate relative influences of natural versus anthropogenic impacts together with the role of groundwater contributions along the river course. Disentangling the relative importance of these factors advance the understanding of source-related inputs and at the same time, provide information on the dilution of anthropogenic and weathering inputs in space and time. Regarding the high vulnerability of karst terrains by agricultural land use and anthropogenic pollution, this is of particular interest with regard to the ecological functioning of rivers with large proportions of limestone in their catchment lithology.

STUDY AREA

The study area was located in southern Germany, in Northern Bavaria between the cities of Bamberg, Bayreuth and Nuremberg (Figure 1). The total catchment area of the Wiesent River is 1040 km^2. The source of the Wiesent River is located in the northwest of the catchment area, at the hamlet of Steinfeld at 445 meters above sea level (m.a.s.l.). From this point the river flows in a southeast to south direction. Near the town of Goeßweinstein, the general flow direction changes westward until the river finally reaches the Regnitz River at 240 m.a.s.l. The total length of the Wiesent River is 72.4 km and the most important tributaries are the rivers Kainach, Truppach, Puettlach, Aufsess, Leinleiter, and Trubach

(Figure 2). Two discharge gauges are located along the main river at the villages of Hollfeld and Muggendorf. They show averaged long-term discharge values of 1.04 $m^3 s^{-1}$ and 7.11 $m^3 s^{-1}$, respectively (LfU, 2014).

The study area is located in a karst region with lithologies of calcites and dolomites that are occasionally interbedded with marly layers. These sediments form the Franconian Jura uplands, which belong to the Franconian Alb that is part of the South German Scarplands. Overall, late Jurassic carbonates cover the majority (~67%) of the catchment area (Figure 2). These comprise a limestone sequence of up to 200 m thickness that is in part dolomitized, and forms a typical karst landscape of the area with incised rivers and other dry valleys, dolines and caverns. This carbonate sequence is overlain by relict patches of Late Cretaceous sandstone with interbedded marl and shale layers.

All sedimentary layers dip at a shallow angle in an eastward direction. As a consequence, lower Jurassic and Late Triassic sandstones and claystones that underlie the thick Late Jurassic carbonate succession crop out in the south-western part of the catchment. Additional sandstone and claystone lithologies of the same Triassic sequence also appear in the eastern part of the main basin, in subcatchments of the tributaries Truppach and Puettlach. Here, the sandstones and claystones were lifted to the surface along a northwest-southeast striking fault.

The vegetation in the south-western part of the catchment is characterized by broad-leaved forest dominated by beeches and scattered small fruit orchards. Coniferous trees largely forest northern and central parts of the catchment, while the eastern regions consist of grassland pastures. Numerous small villages are present in the basin and, particularly in the downstream part of the catchment, agriculture plays an important role in land use.

METHODS

Eight locations (sites 1 to 8 in Figure 2) were sampled during eight field campaigns between January and November 2010 in order to cover all seasons. Starting in April 2010, the six most important tributaries were additionally sampled during the last six sampling campaigns. All tributaries were sampled near their confluences with the Wiesent River (sites 9 to 14 in Figure 2), with water samples collected manually from the middle of the rivers. All bottles were rinsed several times with sample water before filling. Samples destined for major ion analyses were filled without headspace in double closure 100 mL high-density polyethylene bottles with an inner stopper (product item LR100-2, Gosselin SAS, Borre, France). These were then stored in the dark and at 4°C until analysis.

Measurements of temperature, pH, electrical conductivity (EC), and dissolved oxygen (DO) were conducted in the field by a multi parameter instrument (WTW Multi 350i, WTW GmbH, Weilheim, Germany). All probes were calibrated prior to each field campaign. The pH and conductivity probes used built-in automatic temperature compensation functions, and temperature precision is quoted as ± 0.1 °C by the manufacturer. Conductivity values were referenced to 25 °C by a non-linear correction function (nLF) for natural waters. For pH measurements precision was better than ± 0.05 pH units (1σ) and for conductivity determinations it was better than ± 5 µS cm^{-1}. Dissolved oxygen was determined by a galvanic sensor and automatically corrected for ambient air pressure by a built-in pressure sensor.

Total alkalinity (TA) was determined from 100 mL water samples directly in the field by a Hach Digital Titrator (Model 1690001, Hach Company, Loveland, CO, USA). The titration endpoint was determined by colour changes of a pH indicator (bromcresol green-methyl red). At a pH < 9, hydroxide (OH^-) does not contribute to TA at an appreciable concentration and

other TA contributing species (BOH_4^-, $H_3SiO_4^-$) can be regarded as negligible in the waters examined by this study. Therefore, TA essentially contains only carbonic alkalinity and the titration value was used for the calculation of carbonate species concentrations, which is mainly bicarbonate (HCO_3^-) in the observed pH range (see Verma *et al.*, 2015)

Major cations (Na^+, K^+, Li^+, NH_4^+, Ca^{2+}, Mg^{2+}) and anions (F^-, Cl^-, NO_3^-, NO_2^-, SO_4^{2-}, PO_4^{3-}) were determined by ion chromatography (ICS 2000, Thermo Dionex, Sunnyvale, CA, USA). Prior to ion chromatography analysis, samples were filtered with 0.45 µm disk filters, which were flushed with sample before the autosampler vials were filled. Limit of quantification (LOQ) for major ions was 0.1 mg L^{-1} with a typical precision of <5% (1σ) relative standard deviation (RSD) based on the repeated analysis of two control standards treated as unknowns in the lower and upper calibration range. Typical charge errors derived from equivalent concentrations of ion chromatography and field titration data were between 5 and 12%.

RESULTS

Major ion chemistry of the Wiesent River

Major ion concentrations and the described trends along the river course are shown in Figure 3. Detailed analytical data are available in the supplementary material to this article from the website of the host journal, and are additionally archived in PANGAEA.[†]

Calcium showed the highest concentrations amongst all cations, followed by magnesium, sodium, and potassium. Lithium concentrations were always below LOQ (<0.1 mg L^{-1}). Ammonium was detected in only two samples during February, with values of 0.11

[†] www.pangaea.de (DOI for data set pending)

and 0.28 mg L^{-1}, and was below the limit of detection (LOD) in all others. In contrast to most other parameters, calcium and magnesium concentrations showed little variability at the source during the various sampling campaigns, although their general downstream patterns were almost identical for all sampling campaigns. Calcium exhibited a range of 90 to 145 mg L^{-1}, whereas magnesium concentrations ranged between 15 and 45 mg L^{-1} (Figure 3). Calcium concentrations showed an initial decrease between the source and sampling site 2, whereas magnesium increased within the same direction. Further downstream, calcium concentrations remained fairly stable and ranged between 105 and 130 mg L^{-1}, with exception of the November campaign that was characterized by lower values further downstream. After the initial rise, magnesium concentrations tended to decrease until sampling site 4 and showed only minor variations thereafter. In particular, magnesium concentrations showed a clear correlation with corresponding conductivity values for different sampling campaigns, which in turn were correlated with precipitation events and resulting increased discharge values (data shown in van Geldern *et al.*, 2015). This trend was also obvious to a lower extent for calcium, especially during the November campaign.

Sodium concentrations ranged from 8 to 15 mg L^{-1}, stabilizing at a value of 11.2 (±0.6) mg L^{-1} at the source followed by a slight initial rise [arithmetic average (±1σ)]. Values declined further downstream to concentrations of about 8 mg L^{-1} at the lower river course. Potassium concentrations increased from 1.04 (±0.24) mg L^{-1} at the source to values of around 2.0 mg L^{-1} downriver. Maximum values of 3.5 mg L^{-1} were recorded during the November sampling campaign at site 4 and also at locations further downstream. Note that during this campaign most other parameters, as for example calcium and magnesium concentrations or conductivity, showed lower values, a trend that was most likely related to heavy rains prior to that campaign.

180 The ranking of anions in order of decreasing concentrations at the Wiesent River
181 source was bicarbonate, nitrate, chloride, and sulfate with concentrations of 357 (±7), 29.6
182 (±2.7), 22.7 (±1.6), and 15.8 (±1.5) mg L^{-1}, respectively. Interestingly, the downstream
183 behavior revealed different patterns for these anions. Nitrate showed an almost linear
184 monotonic decline over the river course to 17.6 (±1.6) mg L^{-1} at the final sampling site and
185 bicarbonate decreased to an average of 307 (±22) mg L^{-1}. The lowest bicarbonate values were
186 measured along the lower course during the November sampling campaign. A pronounced
187 decrease was observed after the confluence with the Truppach, whereby bicarbonate
188 concentrations dropped below 250 mg L^{-1} in November. The minimum concentration of 228
189 mg L^{-1} was recorded at site 6, located downstream of the Puettlach tributary. During other
190 campaigns, bicarbonate concentrations along the lower course (site 4 and downstream),
191 ranged from 340 to 280 mg L^{-1} (Figure 3).
192 The chloride downstream evolution was similar to sodium or magnesium, with a
193 distinct increase from the source to sampling site 2 and subsequent decreasing values.
194 Chloride concentrations along the lower course ranged from 15 to 25 mg L^{-1}. In contrast,
195 sulfate behaved similar to potassium with a continuous increase along the Wiesent River up to
196 values of 20 to 30 mg L^{-1} near the mouth of the Wiesent at its confluence to the Regnitz. A
197 larger variability of sulfate could be observed downstream of sampling site 4. Here, maximum
198 concentrations of up to 42 mg L^{-1} were recorded during the November sampling campaign.
199 However, an exception from this behavior was observed in February, when the second highest
200 sulfate concentrations were measured at the middle and lower course while the downstream
201 conductivity curve showed maximum values (Figure 3).
202 Low concentrations for fluoride and phosphate above LOD were detected in 12 and 11
203 out of 64 analyses, respectively. When detected, typical concentrations of F^- and PO_4^{3-} were

below 0.3 mg L^{-1} and never exceeded 0.5 mg L^{-1}. Nitrite was not detected in any of the sampling campaigns in the main stem of the Wiesent River (cf. supplementary material)

The tributary and Wiesent River samples are characterized by their major ions in a Piper diagram (Figure 4). Here the tributaries are marked with their numbers in brackets according to Figure 2. The tributaries Kainach (9), Aufsess (11), and Trubach (14) were largely similar to the water chemistry of the main stem of the Wiesent River. The only exception was the Leinleiter tributary (13) with its lower magnesium concentrations, but most other major ion concentrations were similar to those in the main river. Note that the two eastern tributaries Truppach (10) and Puettlach (12) plot differently in Figure 4. For instance, magnesium concentrations were below 12 mg L^{-1} in all samples taken from the Truppach tributary. Morover, both the Truppach and the Puettlach, were characterized by lower bicarbonate, increased potassium, and high sulfate concentrations. These patterns were also transferred to the middle and lower course of the Wiesent River. This was particularly evident after precipitation events, for instance during November. Finally, low concentrations of phosphate (0.11 to 0.72 mg L^{-1})were found during all campaigns in the Truppach and Puettlach, but not in the other tributaries.

DISCUSSION

Geological and anthropogenic controls

The downstream evolution of the parameters discussed above indicates that groundwater is one of the major contributors to the Wiesent River and its tributaries. The expectation is that groundwater infiltration to the river occurs primarily by the piston-flow effect and minor contributions should be derived from overland runoff or soil water. The latter processes are normally observed during snowmelt and more intensive precipitation events. This would particularly hold true for precipitation in tributaries that drain poorly

permeable sediments such as in the eastern part of the catchment (i.e., Truppach and Puettlach). Mixing of these tributary waters with the main river is the most important process for dilution of total dissolved solids (TDS), as indicated by lower conductivity values. In contrast, in the upstream part of the Wiesent Catchment, runoff generation should play a more important role than in permeable karst lithology with fast infiltration rates.

When tributaries are chemically different as compared to the main stem of the Wiesent River, their influences are expected to be obvious. For instance, lower magnesium concentrations in the Truppach likely caused the pronounced drop in magnesium after sampling sites 3 in the Wiesent River. This decline was even more pronounced during periods of low conductivity after precipitation events.

On the other hand, contributions of tributaries that drain a similar lithology as the Wiesent River are harder to detect by natural tracers. For instance, near the catchment outlet, the lithology along the Wiesent River valley changes from carbonate rocks to claystone. The formation is known as the Feuerletten Formation from the Late Trassic. Except for small changes in calcium, magnesium, and sodium the measured parameters did not respond to this prominent change in riverbed lithology. This indicates that groundwater contributions at the final river stretch likely become less important due to the less permeable nature of the underlying thick claystone formation.

At the source of the Wiesent, Ca^{2+}, Mg^{2+}, and HCO_3^- account for 86 % of the TDS and along the river course, this value varies only slightly between 81 and 88 %. This shows that carbonate weathering of calcite ($CaCO_3$) and dolomite ($CaMg(CO_3)_2$) mainly accounts for the high concentrations of these three ions. The stoichiometry of carbonate weathering reactions demands that carbonate-derived calcium and magnesium should be equal to those of bicarbonate when expressed in (milli)equivalents per liter (meq/L). Such a plot of HCO_3^-

252 versus (Ca^{2+} + Mg^{2+}) concentrations reveals a general excess of calcium plus magnesium over
253 bicarbonate (Figure 5A). This excess of cations is partially balanced by Cl^-, SO_4^{2-} and NO_3^-,
254 and suggests that fractions of calcium or magnesium concentrations in the watershed were not
255 exclusively derived from carbonate weathering. Other potential natural sources of calcium are
256 gypsum or silicate weathering of Ca-bearing minerals such as anorthite. However, both
257 minerals are of minor importance in the Jurassic limestone formations and are therefore
258 unlikely candidates for leaching Ca^{2+} and Mg^{2+}.

259 Other sources for this excess include mineral fertilizers that may contain calcium- or
260 magnesium-bearing compounds. This should also correlate with other solutes that are
261 typically derived from these fertilizers, such as nitrate. Further anthropogenic sources that
262 may exist in the watershed include organic fertilizers or domestic sewage. Typical
263 anthropogenic compounds are phosphate, sulfate and nitrogen compounds (NO_3^-, NO_2^-, NH_4^+)
264 from manure and mineral fertilizers. In particular, elevated nitrate concentrations are often
265 related to the use of such fertilizers. During this study, the highest concentrations of nitrate
266 were found at the source of the Wiesent River with a stable value of 29.6 (±2.7) mg L^{-1}. This
267 stability of nitrate concentrations at the source suggests that nitrate may have been
268 continuously transferred into the feeding karst aquifer that acted as a large reservoir.
269 Subsequently, nitrate likely has accumulated over decades and seasonal variations became
270 negligible.

271 This supports the interpretation that the observed excess of calcium and magnesium is
272 a result of long-term anthropogenic influences on the groundwater, particularly at the Wiesent
273 River spring and the upper reaches. It thus indicated the influences from farming activities in
274 the upper part of the catchment. This is surprising, because the Wiesent River has its source in
275 a rural, largely natural region where forests dominate large portions of the catchment and

industry does not play a significant role. Therefore, anthropogenic signals in river water chemistry were expected to be minimal, with inorganic aquatic chemistry mainly mirroring weathering processes or changes in lithology. However, particularly in karst systems, anthropogenic influences may directly enter the river via fast conduit systems and fracture flow.

As opposed to the expected trend of increasing nitrate concentrations further downstream where agriculture and urbanization is more prevalent, a contrary pattern was observed: nitrate concentrations were found to be highest at the source of the Wiesent River (see discussion above) and subsequently decreased with distance from the headwaters during all sampling periods (Figure 3). This pattern further suggests the long-term influences of agricultural land use on the groundwater, particularly in the upstream part of the watershed. Even though agricultural activities are also prevalent in the downstream part of the catchment, their associated nitrate releases may not reach the river as rapidly because the lithology contains a high proportion of fine sandstones and shales that slows or hampers groundwater-related transport to the river.

As for other anthropogenic parameters, road salt and domestic sewage are a primary source of sodium and chloride. Increases in chloride or sodium concentrations were not observed at the source during colder periods. This could either mean that they were dampened in the large feeding karst reservoir or that road salting had a minor influence on the river water chemistry. Since both chloride and potassium showed no distinct seasonality over the entire course or the river, a pronounced influence of this source is likely small in this catchment. It is more likely that these elements reach the river via agricultural activities that are more dominant in the source region, as previously stated. At this juncture, it is unclear why both Cl^- and Na^+ show significant increases from the spring to the second sampling

300 station (site 2) although this trend may be related to the presence of point sources such as
301 sewage release from private housing or farms.
302 Cl^- was also found to be in excess of Na^+ and K^+ and their cation-anion plot does not follow a
303 1:1 ratio (Figure 5B). The Cl^- excess could in part be balanced by excess Ca^{2+} and Mg^{2+} that
304 does not account for carbonate weathering. When assuming that this cation excess stems from
305 fertilizer use in the upstream part of the catchment, it supports the hypothesis that fertilizers
306 are more pronounced in upstream section and may have entered the river via fracture flow of
307 the present karst system.
308 Other fertilizers derived from potash with compounds such as KCl or K_2SO_4 may also
309 have added to the fertilizer load of the river. However, both K^+ and SO_4^{2-} have their lowest
310 values in the source region and show increases further downstream. At first sight, this pattern
311 does not appear to support the hypothesis of more pronounced fertilizer input in the upstream
312 part of the catchment. However, it is possible that both ions actually enter the river as a result
313 of fertilizer transport in the upstream, karst-dominated section of the catchment. The baseline
314 values at the source may then have increased further downstream mainly as a result of K^+ and
315 SO_4^{2-} released from weathering processes in the clay-rich shale formations in the eastern
316 subcatchments, and discharged into the main river stem via tributaries. These and other
317 mechanisms of tributariy influences are discussed in the following section.
318 *Downstream geochemical evolution*
319 After setting of the initial values for physico-chemical parameters at the source, many
320 parameters show changes along the river course. This may be either related to processes that
321 occur within the main river itself such as seasonal temperature changes, or due to the inflow
322 and mixing of waters from different sources.

An important question in river research is the interaction between river water and surface water within the hyporheic and riparian zones along the river course (Krause *et al.*, 2009; Krause *et al.*, 2014). Depending on the hydraulic system, the river can lose water to the groundwater by outflow through the riverbed. This situation is denoted as a losing stream. Alternatively, water from the riparian zone can feed the river, which is denoted as a gaining steam. Different environmental tracers, for example temperature, stable isotopes, or wastewater-related pollutants, have been used to investigate these interactions in detail (Engelhardt *et al.*, 2014; Fox *et al.*, 2016). Furthermore, tributaries with different water chemistry that mix with the main river can also induce changes in water chemistry when differences and fluxes are large enough to cause a measurable shift.

The downstream temperature development of the Wiesent River varies seasonally, with higher temperatures in summer and lower temperatures in winter (Figure 3). Groundwater seeps would shift the warm or cold temperature curve locally towards the average groundwater temperature of about 9 ° C for this region. However, the spatial resolution along the river is not detailed enough to detect point-source groundwater inflow. This is because groundwater temperature can be expected to adjust quickly to the temperature of the river water. Small groundwater contributions would therefore only be detectable close to the point of inflow. However, a steady and spatially ubiquitous groundwater inflow along the whole river course would likely dampen the seasonal changes of the river. Such trends could only be observed at the source and for the remainder of the river it is more likely that groundwater contributions are of minor importance.

A closer examination of the downstream curves showed a notable increase in magnesium concentrations of 7 to 13 mg L^{-1} from the source to sampling site 2 (Figure 3). A larger fraction of dolomite weathering might have increased the portion of magnesium over

calcium. However, this shift was also correlated with increases of sodium and chloride. To a large degree, both elements are likely of anthropogenic origin and this pattern suggests that the Mg^{2+} increase has an anthropogenic component. This is supported by the fact that the increase in chloride was larger than the corresponding increase in sodium, so that chloride could have additionally buffered the magnesium increase. However, even when accounting for Cl^-, a negative charge deficit persisted and Mg^{2+} must have been additionally balanced by other anions. As no other major anions (SO_4^{2-}, NO_3^-) showed a corresponding increase, the surplus of magnesium is most likely buffered by organic compounds that were not measured in this study.

Potassium and sulfate downstream evolutions in the Wiesent River showed opposing patterns as compared to the other major ions along the course (see above). Both ion concentrations gradually increased downstream, whereas other major ion concentrations decreased most likely due to dilution effects by the tributaries Truppach and Puettlach that drain a different lithology. Their lithology is dominated by claystone and sandstone (see Figure 2) and increased concentrations of potassium and sulfate were observed in these two eastern tributaries (supplementary material). A potential anthropogenic source could be potassium sulfate, a common inorganic fertilizer that is often used in fruit orchards. Both ions show a fairly strong correlation in the two subcatchments (Pearson correlation coefficient r = 0.69, p = 0.012) but only about one-tenth of the sulfate is balanced by potassium in this scenario.

One plausible natural source for potassium is weathering of orthoclase and other potassium-bearing silicate minerals in the clastic sediments. As a result of these weathering processes, higher potassium concentrations may have been transported into the Wiesent River.

371 The higher sulfate concentrations could have been caused by the dissolution of
372 gypsum and/or weathering of pyrite. Both minerals are present in the Lower and Middle
373 Jurrasic formations (Krumbeck, 1956; Schröder, 1968) and pyrite is especially abundant in
374 the thick claystone sequence of the 'Amaltheenton' and 'Opalinuston' formation that cover
375 large areas of the eastern subcatchments (Wippern, 1955). The principles of pyrite oxidation
376 follow a sequence of reactions that involve microbiologically-mediated and oxic
377 decomposition of pyrite followed by an anoxic decomposition of pyrite by ferric iron
378 (Lowson, 1982; Evangelou, 1995). The overall stoichiometry is represented by

$$2FeS_2 + 7O_2 + 2H_2O \rightarrow 2Fe^{+} + SO_4^{2-} + 4H^{+}. \quad (1)$$

379 Pyrite weathering reactions release acidity and result in low pH values. However, lower pH
380 values were neither observed in the Wiesent nor in any of the tributaries. This absence of
381 expected pH decrease could be explained by the presence up to 10% carbonates in the
382 claystones (Schröder, 1968). This means that acidity derived from equation (1) could become
383 directly neutralized by reaction with carbonates.
384 Unexpectedly higher concentrations of potassium and sulfate in the Truppach and
385 Puettlach tributaries was observed in November: samples from this month showed increased
386 concentrations of potassium and sulfate that were also found in the middle and lower reaches
387 of the Wiesent River, downstream of the Truppach and Puettlach confluences (Figure 3). In
388 contrast, most other ions (e.g., calcium or magnesium) were diluted. This dilution can be
389 attributed to increased fluxes of low-mineralized surface runoff following a heavier period of
390 rainfall in November. Surface runoff was also expected to also dilute the concentrations of
391 potassium and sulfate. However, the data suggest that potassium and sulfate were largely
392 derived from weathering processes at the land surface or in the soil zone. They were then

393 mobilized and flushed with increased concentrations along the eastern tributaries into the
394 Wiesent River during precipitation events.

395 **CONCLUSIONS**

396 The Wiesent River has an unusual chemical downriver evolution, particularly for
397 solutes that are often derive from agricultural fertilizers. While increased anthropogenic
398 activities normally occur in the downriver sections of the catchment, an unexpectedly stronger
399 fertilizer-derived signal was found in its upstream area. This is particularly true for nitrate.
400 These agricultural inputs may have been introduced through fast conduit and fracture flow in
401 the karst lithology of the upstream catchment. Agricultural influences may even stem from
402 beyond the catchment surface water boundaries. After leaving the source, these inputs became
403 diluted further downstream, specifically via tributaries that were not sourced from carbonate
404 lithologies. While Ca^{2+}, HCO_3^- and NO_3^- decreased over the course of the river, we found
405 increases of K^+ and SO_4^{2-} in the downstream section that is more influenced by clay
406 lithologies. This enables a division of the river into two sections: an upstream part that is
407 dominated by karst and receives strong fertilizer inputs, and a downstream section that
408 receives less groundwater inputs but is subject to increased contributions by tributaries that
409 drain sandstone and shale lithologies. This highlights the importance of including tributaries
410 in river studies.

411 Overall, our findings indicate that bedrock geology remains the dominant control on
412 the major ion chemistry of the Wiesent River, and that agricultural influences are the
413 strongest near the headwaters despite increased land-use further downstream, due to long-
414 term storage and accumulation in karst aquifers. Future studies should include ecological

415 indicators that may be more sensitive to fertilizer input, such as counts of specific organisms
416 and quantification of sediment loads.
417

418 **ACKNOWLEDGMENTS**

419 We thank Irene Wein and Silke Meyer (FAU) for their help with laboratory work.
420 Additional chemical data and discharge values were kindly provided by Michael Lorenz
421 (Wasserwirtschaftsamt Kronach), Nadine Döhler and Joachim Stoermer (Landesamt für
422 Umwelt, LfU). Partial financial support was provided by the Universitätsbund of Friedrich-
423 Alexander-Universität Erlangen-Nürnberg, the grant for major instrumentation to the chair of
424 Applied Geology (INST 90/678-1 FUGG), and by the German Research Foundation (DFG
425 grant BA 2207/6-1).
426
427

References

Barth JAC, Cronin AA, Dunlop J, Kalin RM. 2003. Influence of carbonates on the riverine carbon cycle in an anthropogenically dominated catchment basin: Evidence from major elements and stable carbon isotopes in the Lagan River (N. Ireland). *Chemical Geology* **200**: 203-216.

Brunet F, Potot C, Probst A, Probst JL. 2011. Stable carbon isotope evidence for nitrogenous fertilizer impact on carbonate weathering in a small agricultural watershed. *Rapid Communications in Mass Spectrometry* **25**: 2682-2690. DOI: 10.1002/rcm.5050.

Engelhardt I, Barth JAC, Bol R, Schulz M, Ternes TA, Schüth C, van Geldern R. 2014. Quantification of long-term wastewater fluxes at the surface water/groundwater-interface: An integrative model perspective using stable isotopes and acesulfame. *Science of the Total Environment* **466-467**: 16-25. DOI: 10.1016/j.scitotenv.2013.06.092.

Evangelou VP. 1995. *Pyrite oxidation and its control*. CRC Press; 293.

Fox A, Laube G, Schmidt C, Fleckenstein JH, Arnon S. 2016. The effect of losing and gaining flow conditions on hyporheic exchange in heterogeneous streambeds. *Water Resources Research* **52**: 7460-7477. DOI: 10.1002/2016WR018677.

Gandois L, Perrin A-S, Probst A. 2011. Impact of nitrogenous fertiliser-induced proton release on cultivated soils with contrasting carbonate contents: A column experiment. *Geochimica et Cosmochimica Acta* **75**: 1185-1198. DOI: 10.1016/j.gca.2010.11.025.

Kanduč T, Szramek K, Ogrinc N, Walter L. 2007. Origin and cycling of riverine inorganic carbon in the Sava River watershed (Slovenia) inferred from major solutes and stable carbon isotopes. *Biogeochemistry* **86**: 137-154. DOI: 10.1007/s10533-007-9149-4.

451 Krause S, Boano F, Cuthbert MO, Fleckenstein JH, Lewandowski J. 2014. Understanding
452 process dynamics at aquifer-surface water interfaces: An introduction to the special
453 section on new modeling approaches and novel experimental technologies. *Water*
454 *Resources Research* **50**: 1847-1855. DOI: 10.1002/2013WR014755.
455 Krause S, Hannah DM, Fleckenstein JH. 2009. Hyporheic hydrology: interactions at the
456 groundwater-surface water interface. *Hydrological Processes* **23**: 2103-2107. DOI:
457 10.1002/hyp.7366.
458 Krumbeck L. 1956. *Erläuterungen zur Geologischen Karte von Bayern 1: 25000 - Blatt Nr.*
459 *6232 Forchheim*. Bayerisches Geologisches Landesamt; 80.
460 LfU. 2014. Hochwassernachrichtendienst. Bayerisches Landesamt für Umwelt (LfU).
461 Accessible at http://www.hnd.bayern.de, (last accessed 28 Feb 2014).
462 Lowson RT. 1982. Aqueous oxidation of pyrite by molecular oxygen. *Chemical Reviews* **82**:
463 461-497. DOI: 10.1021/cr00051a001.
464 Meybeck M. 1982. Carbon, nitrogen, and phosphorus transport by world rivers. *American*
465 *Journal of Science* **282**: 401-450. DOI: 10.2475/ajs.282.4.401.
466 Meybeck M. 1993. Riverine transport of atmospheric carbon: Sources, global typology and
467 budget. *Water, Air, and Soil Pollution* **70**: 443-463. DOI: 10.1007/BF01105015.
468 Perrin A-S, Probst A, Probst J-L. 2008. Impact of nitrogenous fertilizers on carbonate
469 dissolution in small agricultural catchments: Implications for weathering CO2 uptake
470 at regional and global scales. *Geochimica et Cosmochimica Acta* **72**: 3105-3123.
471 DOI: 10.1016/j.gca.2008.04.011.
472 Richey JE, Melack JM, Aufdenkampe AK, Ballester VM, Hess LL. 2002. Outgassing from
473 Amazonian rivers and wetlands as a large tropical source of atmospheric CO2.
474 *Nature* **416**: 617-620.

475 Schröder B. 1968. *Erläuterungen zur Geologischen Karte von Bayern 1:25000 - Blatt Nr.*
476 *6332 Erlangen Nord*. Bayerisches Geologisches Landesamt; 159.
477 Stögbauer A, Strauss H, Arndt J, Marek V, Einsiedl F, van Geldern R. 2008. Rivers of North-
478 Rhine Westphalia revisited: Tracing changes in river chemistry. *Applied*
479 *Geochemistry* **23**: 3290-3304. DOI: 10.1016/j.apgeochem.2008.06.030.
480 van Geldern R, Schulte P, Mader M, Baier A, Barth JAC. 2015. Spatial and temporal
481 variations of pCO_2, dissolved inorganic carbon and stable isotopes along a temperate
482 karstic watercourse. *Hydrological Processes* **29**: 3423-3440. DOI:
483 10.1002/hyp.10457.
484 Verma MP, Portugal E, Gangloff S, Armienta MA, Chandrasekharam D, Sanchez M,
485 Renderos RE, Juanco M, van Geldern R. 2015. Determination of carbonic species
486 concentration in natural waters - Results from a worldwide proficiency test.
487 *Geostandards and Geoanalytical Research* **39**: 233-255. DOI: 10.1111/j.1751-
488 908X.2014.00306.x.
489 Wippern J. 1955. *Erläuterungen zur Geologischen Karte von Bayern 1: 25000 - Blatt Nr.*
490 *6134 Waischenfeld*. Bayerisches Geologisches Landesamt; 47.
491 Yang C, Telmer K, Veizer J. 1996. Chemical dynamics of the "St. Lawrence" riverine
492 system: δD_{H2O}, $\delta^{18}O_{H2O}$, $\delta^{13}C_{DIC}$, $\delta^{34}S_{sulfate}$, and dissolved $^{87}Sr/^{86}Sr$. *Geochimica et*
493 *Cosmochimica Acta* **60**: 851-866. DOI: 10.1016/0016-7037(95)00445-9.
494

FIGURE CAPTIONS

Figure 1. Location of the study area in Southern Germany. The total area of the Wiesent Catchment is 1040 km^2.

Figure 2. Sampling points and lithology of the Wiesent catchment. The upper and central parts of the catchment are dominated by Late Jurassic limestone formations, whereas Late Triassic to Middle Jurrasic claystones and sandstones emerge in the southwestern and eastern part of the catchment that lie further downstream. Sampling points are indicated for the Wiesent main river (numbers in circles) and tributaries (numbers in square boxes).

Figure 3. Major ion chemistry, electric conductivity (EC), and temperature (T) along the Wiesent River for bi-monthly sampling campaigns. Bicarbonate was calculated from total alkalinity (TA) field titration assuming that TA is comprised by carbonic species only and CO_3^{2-}-contributions are negligible at the observed pH values. Other major ion concentrations were determined by ion chromatography.

Figure 4. Piper diagram for the Wiesent River and sampled tributaries. Numbers in parentheses refer to sampling locations. The tributaries Truppach (10) and Puettlach (12) mainly drain claystone and sandstone dominated lithology. These tributaries are characterized by lower magnesium, increased potassium and higher sulfate concentrations. This different water chemistry could also have been caused by anthropogenic inputs.

Figure 5. (A) Bicarbonate plotted against calcium plus magnesium concentrations of the Wiesent River expressed in meq L^{-1}. The dashed line indicates the stoichiometric relation of

519 carbonate weathering. (B) Chloride versus sodium plus potassium expressed in meq L^{-1}. The
520 dashed line indicates the stoichiometric relationship for salt dissolution.

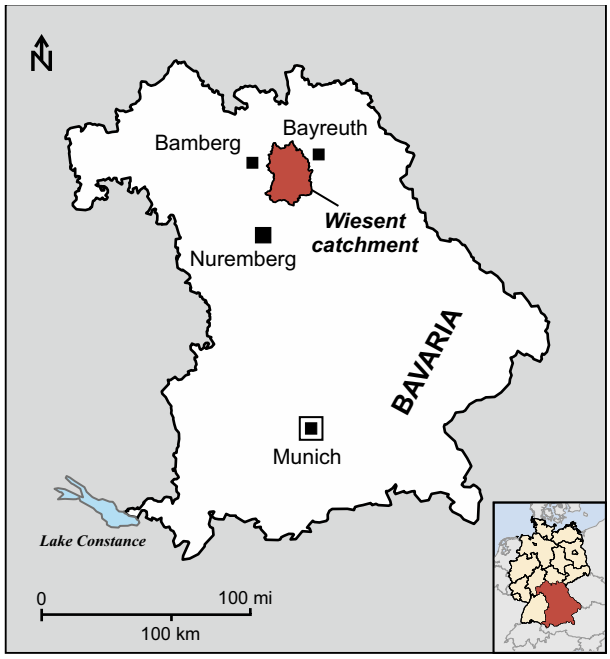
N
Bamberg
Bayreuth
Wiesent
catchment
Nuremberg
BAVARIA
Munich
Lake Constance
0
100 mi
100 km

Figure 1

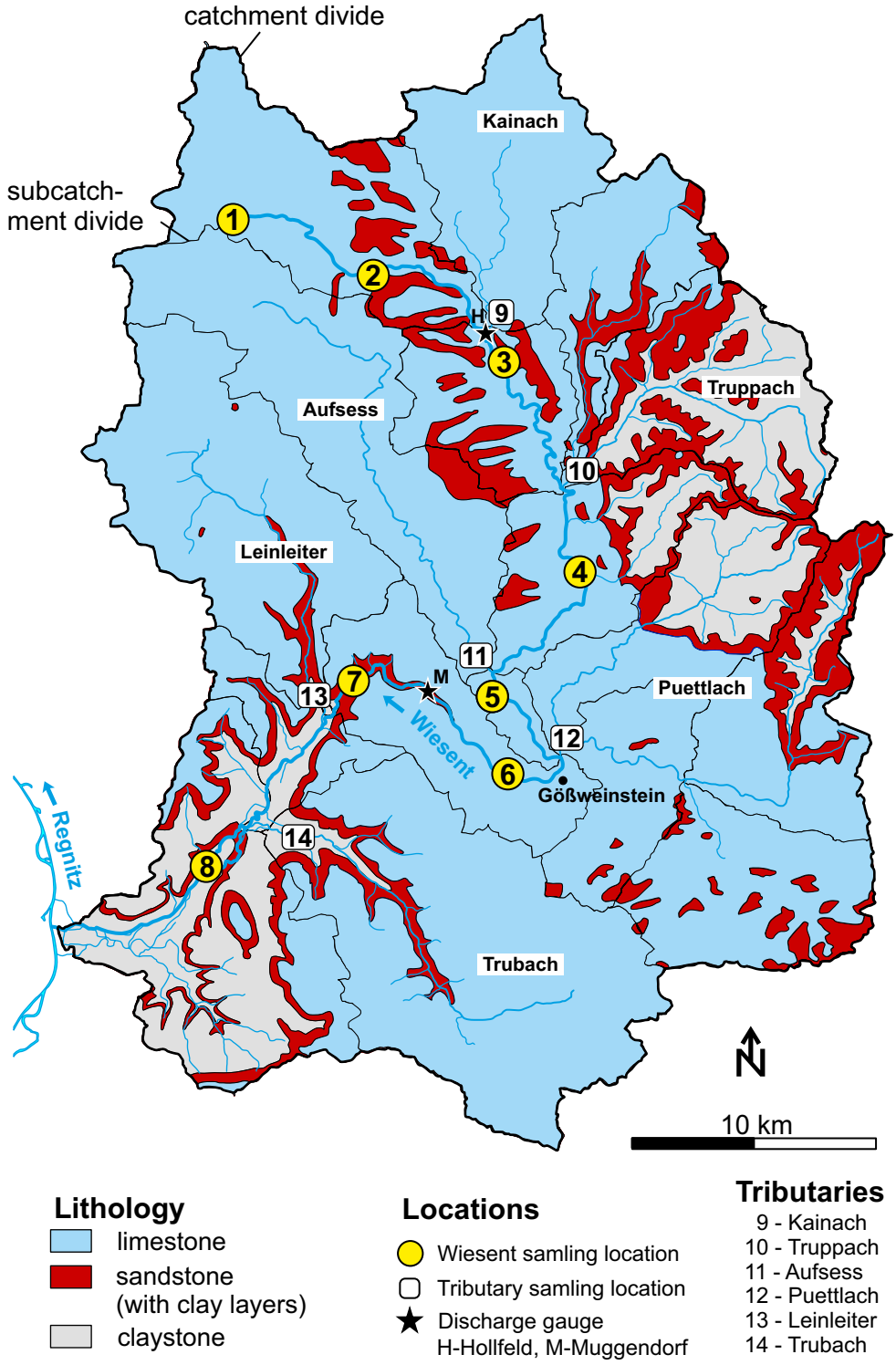
catchment divide
subcatch-
ment divide
Kainach
Truppach
Aufsess
Leinleiter
Puettlach
Trubach
Gößweinstein
Wiesent
Regnitz
H
M
1
2
3
4
5
6
7
8
9
10
11
12
13
14
10 km
Lithology
limestone
sandstone
(with clay layers)
claystone
Locations
Wiesent samling location
Tributary samling location
Discharge gauge
H-Hollfeld, M-Muggendorf
Tributaries
9 - Kainach
10 - Truppach
11 - Aufsess
12 - Puettlach
13 - Leinleiter
14 - Trubach

Figure 2

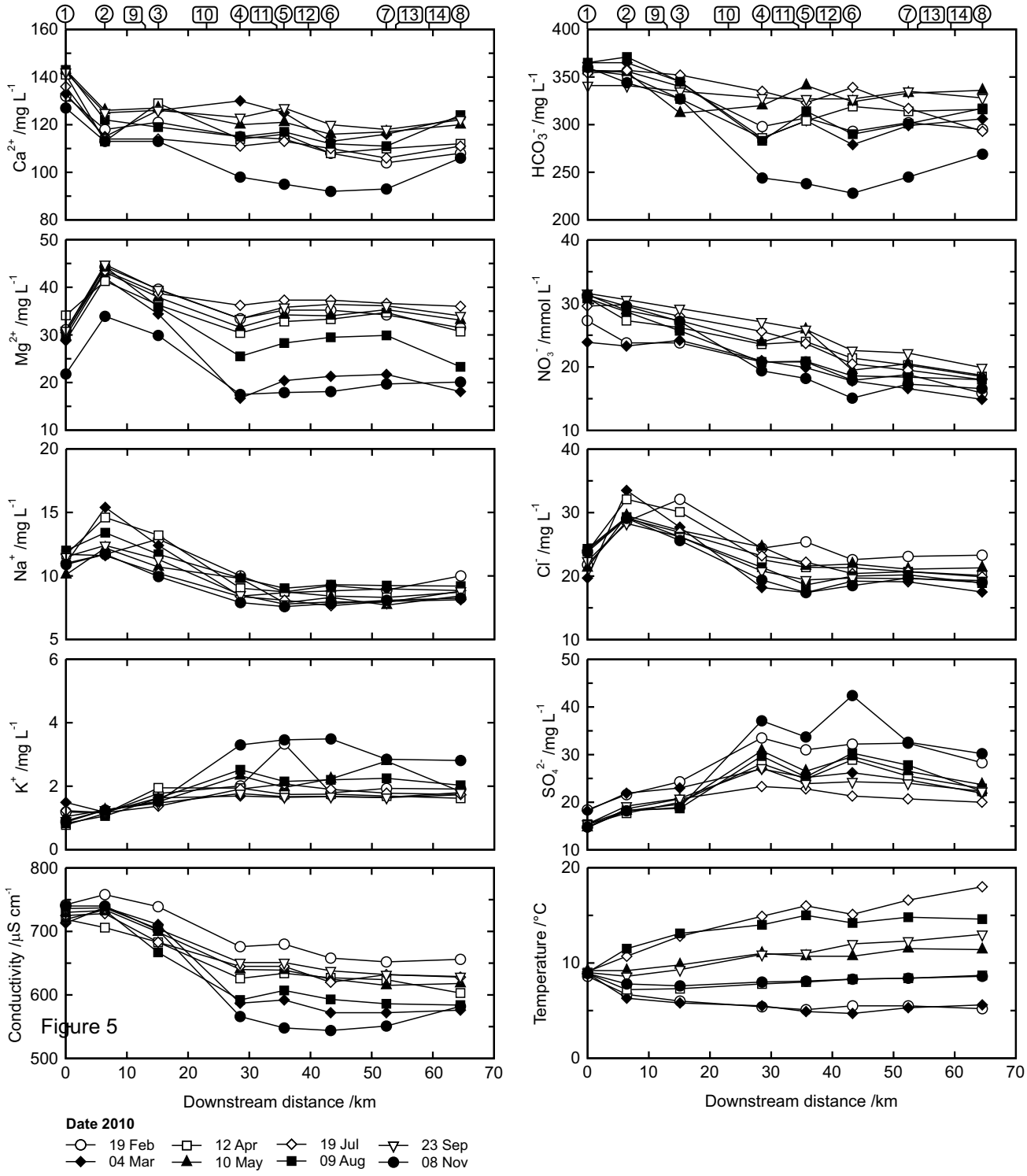

Figure 5

Figure 3

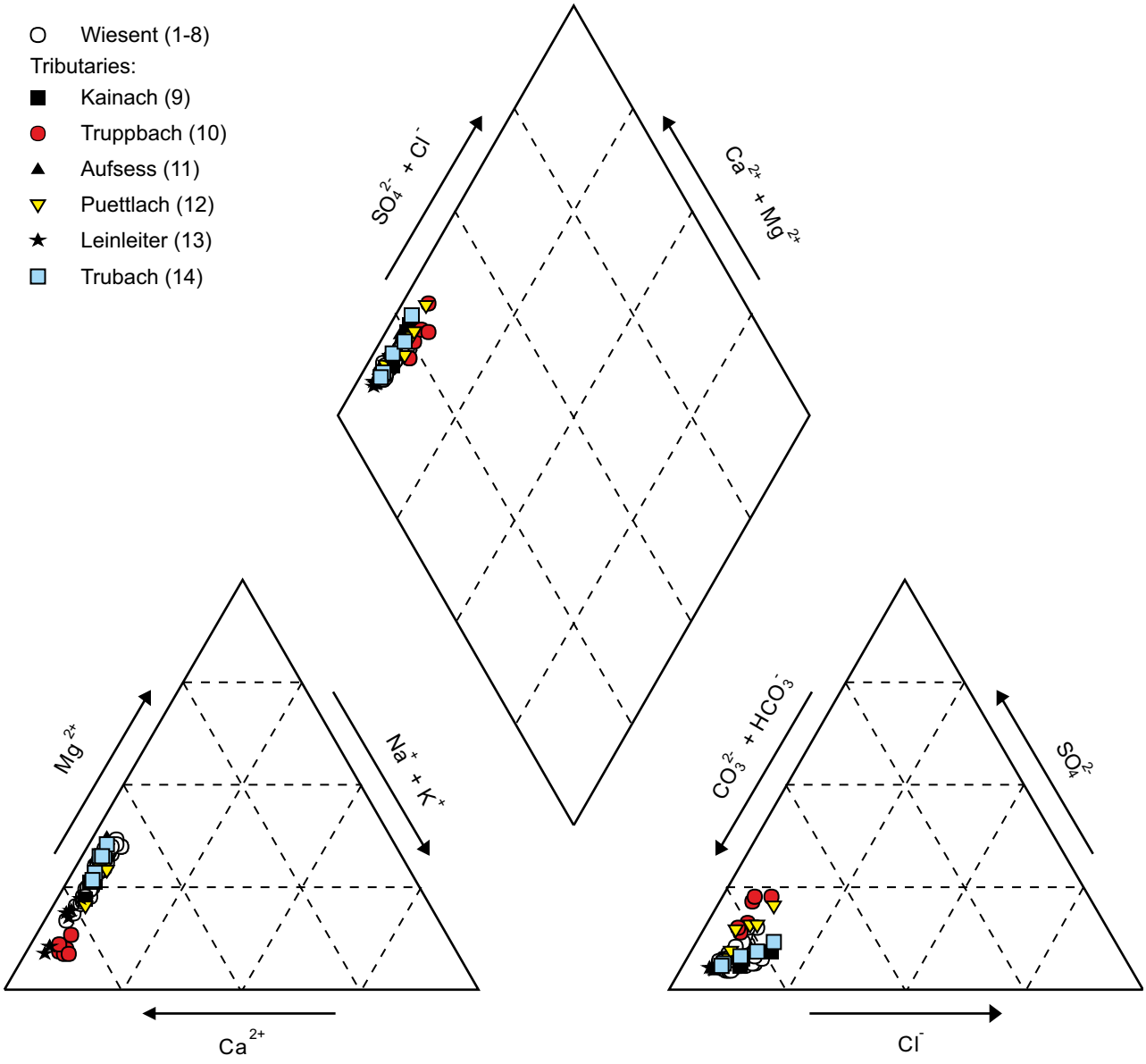
Wiesent (1-8)
Tributaries:
Kainach (9)
Truppbach (10)
Aufsess (11)
Puettlach (12)
Leinleiter (13)
Trubach (14)
SO4 2- + Cl-
Ca 2+ + Mg 2+
Mg 2+
Na+ + K+
Ca 2+
CO3 2- + HCO3-
SO4 2-
Cl-

Figure 4

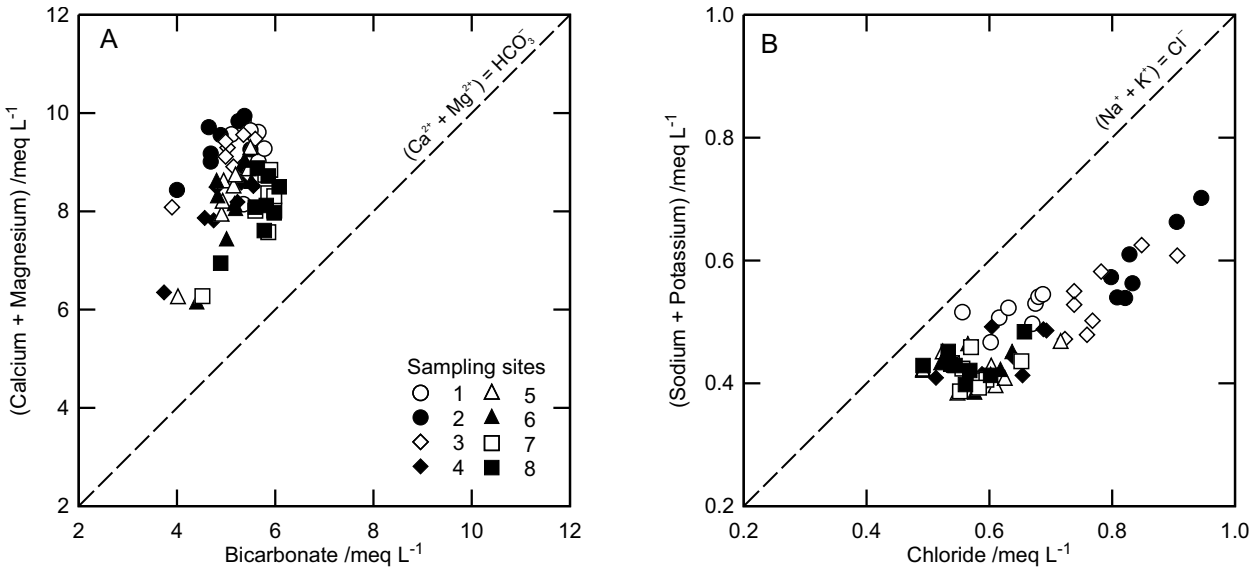
A
B
(Calcium + Magnesium) /meq L-1
Bicarbonate /meq L-1
(Sodium + Potassium) /meq L-1
Chloride /meq L-1
(Ca2+ + Mg2+) = HCO3-
(Na+ + K+) = Cl-
Sampling sites
1
2
3
4
5
6
7
8

Figure 5